X-Ray Photoemission Cross-Section Modulation in Diamond, Silicon, Germanium, Methane, Silane, and Germane*

R. G. Cavell,† S. P. Kowalczyk, L. Ley,‡ R. A. Pollak,§ B. Mills, D. A. Shirley, and W. Perry
Department of Chemistry and Lawrence Berkeley Laboratory, University of California, Berkeley, California 94720
(Received 27 November 1972)

The high-resolution x-ray-photoemission-spectroscopy (XPS) valence-band spectrum from a cleaved natural-diamond single crystal is reported. The absence of extrinsic structure allows a reliable comparison with band theory. The XPS molecular-orbital spectra of methane, silane, and germane are also given. The modulation of photoelectric cross sections in the valence bands of diamond, Si, and Ge are discussed and compared with atomic XPS cross sections derived from the spectra of CH_4, SiH_4, and GeH_4.

The allotropic form of carbon, diamond, is the prototype for group-IV crystals of the diamond structure. Many calculations of the energy-band structure have been carried out,[1] yielding results that vary more widely than is the case for its congeners, silicon, and germanium. Thus, it is especially desirable to determine the positions of the diamond energy bands experimentally. In this paper, we report the total valence-band density-of-states spectrum of a cleaved single crystal of diamond. The spectrum was obtained using x-ray photoemission spectroscopy (XPS), which has recently been employed to yield total valence-band spectra for silicon and germanium.[2] The diamond spectrum is compared with theory and with the XPS molecular-orbital spectra of CH_4, SiH_4, and GeH_4.

A diamond single crystal was cleaved in a dry N_2 atmosphere, introduced into the analyzer chamber of an HP 5950A electron-spectroscopy-for-chemical-analysis (ESCA) spectrometer at 8×10^{-9} Torr, and irradiated with monochromatized Al$K\alpha_{1,2}$ radiation.[3]

Previous XPS studies of diamond[4,5] on powdered samples yielded valence-band spectra that were not intrinsic, and no detailed comparisons with band-structure theory were possible. In a preliminary experiment on an untreated diamond single crystal, we observed a valence-band spectrum that was similar to the previously reported spectra.[4,5] After cleaving the diamond the C(1s)/O(1s) ratio rose from 4 to 13, and the valence-band spectrum showed no evidence of oxygen contamination.

The uncorrected spectra $I(E)$ of the diamond valence band and the diamond C(1s) core region are shown in Fig. 1. Assuming the satellite structure of the C(1s) line to be extrinsic, we corrected the valence-band spectrum quantitatively for inelastic losses. The corrected spectrum $I'(E)$ is shown in Fig. 2. This correction does not appreciably affect the valence-band structure below 25-eV binding energy.

A thin layer of gold was evaporated onto the diamond crystal after the valence-band measurements were completed, and the separation of the Au-$4f_{7/2}$ and the underlying diamond C(1s) lines was measured. The binding energy of the Au-$4f_{7/2}$ line relative to the Fermi edge in gold metal was measured to be 84.00 ± 0.01 eV. Using this, the diamond C(1s) binding energy relative to the Fermi level of a thin surface film of gold is 284.44 ± 0.07 eV, in fair agreement with the value 284.0 ± 0.3 eV reported by Thomas *et al.*[4]

There are three peaks in $I'(E)$ as was the case for Si and Ge,[2] which are also shown in Fig. 2 for comparison. The wider spacing of $I'(E)$ for diamond is consistent with theoretical expectations[1] and is due to the smaller lattice constant in diamond. With two atoms per unit cell and four electrons per atom, diamond has four doubly occupied valence bands, as indicated in Fig. 3. These bands produce three peaks in the density of states $\rho(E)$,

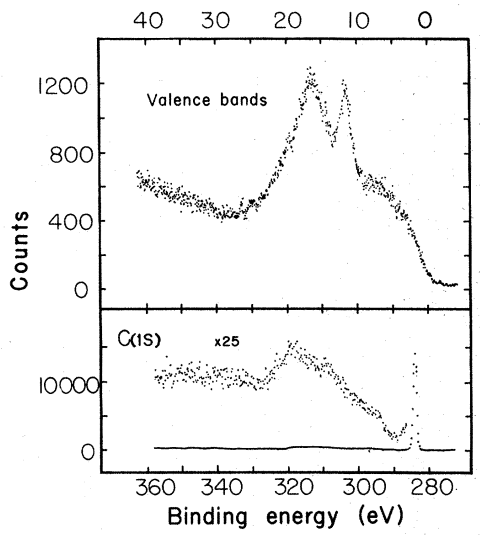

FIG. 1. XPS valence band (upper curve) and C(1s) core region (lower curve) of diamond.

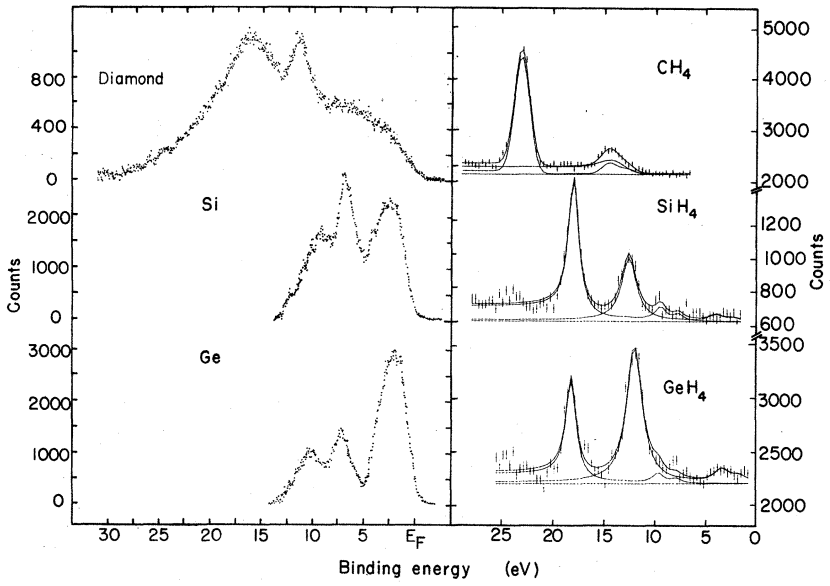

FIG. 2. (a) Corrected valence-band spectra $I'(E)$ for diamond, Si, and Ge; (b) molecular orbitals for CH_4, SiH_4, and GeH_4. The $K\alpha_{3,4}$ satellites in these spectra are accounted for in the least-squares computer fit.

with the top two bands forming a single peak. Labeling the $I'(E)$ peaks as I, II, and III (Fig. 3), we identify most of peak I with band 1, peak II with band 2, and peak III with bands 3 and 4.

In a one-electron picture we have, to a good approximation,

$$I'(E) \propto \rho(E)\,\sigma(E, h\nu)\,\rho_e(h\nu - E)\ .$$

Here $\rho(E)$ is the valence band and $\rho_e(h\nu - E)$ the continuum density of states, and $\sigma(E, h\nu)$ is the photoemission cross section. Taking $\rho_e(h\nu - E)$ as constant over the valence-band width ΔE, since[6] $h\nu \gg \Delta E$, we have

$$I'(E) \propto \rho(E)\,\sigma(h\nu, E)\ ,$$

and detailed comparison of $I'(E)$ with $\rho(E)$ would require knowledge of $\sigma(h\nu, E)$.

For molecules, cross-section modulation is readily understood.[7] The cross section is proportional to the square of the overlap between the initial one-electron state and the continuum final state of the electron,

$$\sigma(h\nu, E) \propto \left|\langle \psi_i(E) \left| \chi_f(h\nu - E)\right\rangle\right|^2\ .$$

Taking $\chi_f(h\nu - E)$ as a plane wave, the de Broglie wavelength of an electron ejected from the valence bands by Al$K\alpha$ radiation is 0.32 Å. Thus, the major contributions to $\sigma(h\nu, E)$ must come from those regions in which $\psi_i(E)$ has a curvature corresponding to this wavelength i.e., the atomiclike regions near the nucleus. The carbon 2*s* orbital has a larger cross section for photoemission at this energy than the carbon 2*p* orbital, because its radial node makes the curvature of the 2*s* wave functions similar to that of the photoelectron.

Comparison of Figs. 2 and 3 reveals that cross-section modulation is very important in diamond, Si, and Ge. The valence-electron wave functions are of course eigenfunctions of *linear* momentum

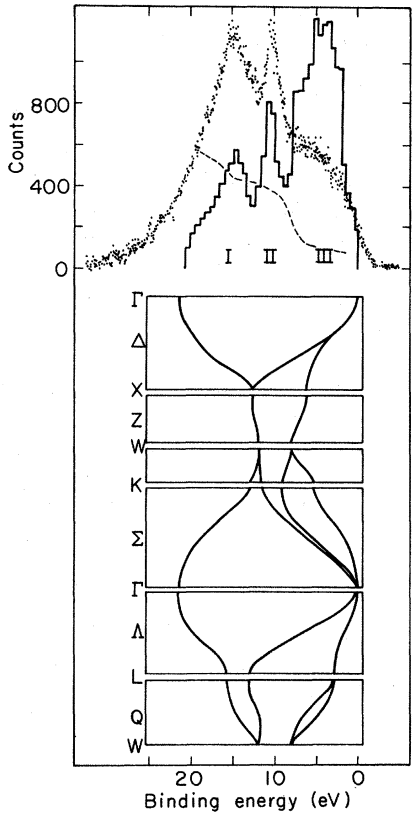

FIG. 3. Comparison of the calculated density of states (Ref. 12) with $I'(E)$ for diamond. The broken line gives the cross-section modulation as obtained by dividing $I'(E)$ into $\rho(E)$.

TABLE I. Binding energies E_B and widths [full width at half-maximum (FWHM)] of molecular orbitals of methane, silane, and germane. Energies in eV. Binding energies were measured using neon as a standard. The Ne(2s) peak was assigned a value of 48.72 eV.

Orbital	CH_4	SiH_4	GeH_4
A_1			
E_B	23.08(4)	18.01(4)	18.46(4)
FWHM	1.71(3)	1.16(6)	1.17(6)
T_2			
E_B	14.5(2)	12.67(4)	12.28(4)
FWHM	2.8(5)	1.69(6)	1.75(6)

rather than *angular* momentum because of the lattice periodicity. Expansion into atomic orbitals therefore extends over the whole Hilbert space that is orthogonal to the ion cores. However—especially near the nucleus—the largest contributions to this expansion come from the ns and np orbitals, where n is the principal quantum number of the valence electrons in C, Si, and Ge, respectively. In this sense band 1 is mostly s like and bands 3 and 4 are mostly p like.[8] Band 2 is a mixture of s- and p-like functions. The variation in the peak area ratio (I+II)/III should therefore correspond to a similar variation in the atomic-orbital cross-section ratio $\sigma(s)/\sigma(p)$, as noted earlier for Si and Ge.[2]

To investigate this point more quantitatively we obtained XPS spectra of the valence regions of the gaseous compounds methane (CH_4), silane (SiH_4), and germane (GeH_4) in the Berkeley iron-free spectrometer, using a Mg$K\alpha_{1,2}$ x-ray source. The latter two gases were prepared applying the techniques of Refs. 9 and 10. In all three cases the spectra (Fig. 2 and Table I) exhibit two peaks which correspond to the (s-like) A_1 level and the (p-like) T_2 level.

A linear-combination-of-atomic-orbitals (LCAO) calculation for the three molecules yields the parentages of the two levels in terms of the atomic s and p orbitals. From these parentages and the measured peak intensities we deduced the ratios $\sigma(ns)/\sigma(np)$ listed in Table II. These ratios show a dramatic change from C to Ge, thus accounting for the intensity variation of peaks I, II, and III in the valence-band spectra of the elements (a comparison of Al$K\alpha$ and Mg$K\alpha$ spectra is valid because cross-section ratios vary little between these photon energies[11]). In fact, the atomic ratios show more variation because the valence bands in the solids do not have pure s or p character. Even in the tight-binding approach the states which make

TABLE II. Comparison of the atomic cross-section ratio for photoemission $\sigma(s)/\sigma(p)$ with the intensity ratio of peaks I+II to peak III in the valence-band spectra of diamond, Si, and Ge.

	(I+II)/III	$\sigma(s)/\sigma(p)$
C	2.9 ± 0.3	12
Si	1.6 ± 0.2	3.4
Ge	0.7 ± 0.1	1.0

up $\rho(E)$ are mixtures of the s and p basis functions for every value of E. This mixture alone tends to equalize the cross section over the valence region. It is thus clear that cross-section modulation can slightly shift the apparent positions of characteristic features from $\rho(E)$ to $I'(E)$.

At Γ, the center of the Brillouin zone, bands 2–4 all have p character. Since they all approach Γ_{25}' with zero slope, the density of states falls rather sharply at this energy—the top of the valence bands. Thus, in principle, $E(\Gamma_{25}')$ could be determined rather accurately, without ambiguity due to s,p mixing or unfavorable structure in $\rho(E)$. By extrapolating down from the steepest part of the peak III, we obtained $E(\Gamma_{25}') = 1.8 \pm 0.3$ eV relative to E_F(Au).

The peaks in $I'(E)$ should fall at maxima in $\rho(E)$ with small shifts between the two sets of maxima arising from instrumental broadening of unsymmetrical peaks and from s/p mixing. The over-all increase of s character with energy below E_F tends to bias $I'(E)$ downward in energy relative to $\rho(E)$. With these factors considered, we assign the positions of peaks I and II as 17.9 ± 0.2 and 13.2 ± 0.1 eV below E_F(Au), respectively.

The upper portion of Fig. 3 compares the calculated $\rho(E)$ of Painter, Ellis, and Lubinsky[12] with our $I'(E)$. Their band structure is shown in the lower portion of Fig. 3. Since $\rho(E)$ and $I'(E)$ show excellent agreement in the positions of all characteristic features, it is valid to deduce the variation of $\sigma(E)$ over the valence region, as indicated by the broken line in Fig. 3. This line exhibits the smooth decrease from the bottom of the valence band to its top, as expected from the discussion given above. Thus the relative intensities in photoelectron spectra can provide a valuable tool in exploring the atomic origin of different regions in the valence bands of solids.

The award of a grant (to L. L.) by the Max-Kade Foundation and sabbatical-leave assistance (to R. G. C.) from the University of Alberta are gratefully acknowledged.

*Work performed under the auspices of the U. S. Atomic Energy Commission.

†On leave from University of Alberta (1971–1972).

‡On leave from University of Bonn, Germany.

§In partial fulfillment of Ph.D.

[1]Detailed references to the early literature appear in Refs. 4

and 5 below.
[2]L. Ley, S. Kowalczyk, R. A. Pollak, and D. A. Shirley, Phys. Rev. Lett. **29**, 1088 (1972).
[3]R. A. Pollack, S. Kowalczyk, L. Ley, and D. A. Shirley, Phys. Rev. Lett. **29**, 274 (1972).
[4]J. M. Thomas, E. L. Evans, M. Barber, and P. Swift, Trans. Faraday Soc. **67**, 1875 (1972).
[5]T. Gora, R. Staley, J. D. Rimstidt, and J. Sharma, Phys. Rev. B **5**, 2309 (1972).
[6]C. S. Fadley and D. A. Shirley, J. Res. Natl. Bur. Stand. (U.S.) **74A**, 543 (1970).
[7]U. Gelius, *Electron Spectroscopy*, edited by D. A. Shirley (North-Holland, Amsterdam, 1972) p. 311.
[8]J. P. Walter and Marvin L. Cohen, Phys. Rev. B **4**, 1877 (1971).
[9]A. D. Norman, J. R. Webster, and W. L. Jolly, Inorg. Synth. **11**, 170 (1968).
[10]W. L. Jolly, *The Synthesis and Characterization of Inorganic Compounds* (Prentice-Hall, Englewood Cliffs, N.J., 1970), p. 496.
[11]K. Siegbahn, C. Nordling, G. Johansson, J. Hedman, P. F. Hedín, K. Hamrin, U. Gelius, T. Bergmark, L. O. Werme, R. Manne, and F. Baer, *ESCA Applied to Free Molecules* (North-Holland, Amsterdam, 1969), p. 40.
[12]G. S. Painter, D. E. Ellis, and A. R. Lubinsky, Phys. Rev. B **4**, 3610 (1971).

PHYSICAL REVIEW B VOLUME 7, NUMBER 12 15 JUNE 1973

Low-Temperature Lattice Thermal Conductivity of GaSb-InSb Alloys

K. C. Sood and G. S. Verma
Physics Department, Banaras Hindu University, Varanasi-5, India
(Received 5 May 1972)

It has been shown in the present work that the large contribution to the lattice thermal resistivity of GaSb-InSb alloys in the temperature range 4–10 °K comes from the phonon scattering by holes which are associated with the acceptor defects. The increase in the low-temperature lattice thermal conductivity with the increase of InSb concentration has been explained on the basis that the density-of-states effective mass of the holes decreases as the InSb concentration is increased in the alloy.

I. INTRODUCTION

GaSb is unusual in the sense that its low-temperature lattice thermal conductivity[1] is about 100 times smaller than its expected value from the boundary scattering of phonons only. Further, it has been observed by Briggs[2] that at liquid-helium temperatures, the lattice thermal conductivity of GaSb increases when it is alloyed with InSb. These results suggest that pure GaSb must contain some extra scattering centers which are neutralized when it is mixed with InSb.

Recently, Briggs and Challis[3] have proposed that the acceptor defects, which are present in GaSb due to nonstoichiometry,[4] act as scattering centers to give the extra thermal resistivity. Since InSb is free from such defects, it decreases the defect concentration when mixed into GaSb, and consequently the number of scattering centers also decreases. At low temperatures the phonon scattering by defects dominates over other scatterings and so an increase in the lattice thermal conductivity is expected when GaSb is alloyed with InSb. Briggs and Challis[3] are, however, uncertain about the mechanism by which the phonons are scattered by acceptor defects. The scattering may be caused by either holes associated with the acceptor defects or the aggregated defects.

In the present paper, we have tried to investigate to what extent the holes, associated with the acceptor defects, are responsible for the scattering of phonons. Since GaSb contains a high number of acceptor defects, the associated holes are considered to be free in the present work, and Ziman's[5,6] theory has been used for the hole-phonon scattering cross section. The density-of-states effective mass, which appears in the hole-phonon relaxation rate, has been varied with InSb concentration to give a theoretical explanation of the experimental results[2,3] of lattice thermal conductivity in GaSb-InSb alloys in the temperature range 4–10 °K. We suggest that the variation of the density-of-states effective mass with InSb concentration is due to the change in the band structure of the GaSb-InSb system with composition. Since the aim of the present paper is confined to the investigation of the role of phonon-hole scattering in the phonon-conductivity results of InSb-GaSb alloys, the calculations are limited to only up to 10 °K. Because of the cutoff factor due to momentum-conservation considerations, phonon-hole scattering is effective only below 10 °K.

There is another important aspect of the present problem. While alloying with InSb, not only is the concentration of acceptor defects decreased but also the point-defect concentration is increased. Such an increase in the concentration of point defects leads to a decrease in the lattice thermal conductivity. Such effects are usually more noticeable at temperatures beyond the conductivity maxi-